JOURNAL OF MATERIALS SCIENCE 29 (1994) 1575–1580

# Growth of tubular boron nitride filaments

P. GLEIZE, M. C. SCHOULER, P. GADELLE*, M. CAILLET
*Laboratoire Science des Surfaces et Matériaux Carbones, URA CNRS n° 413, Institut National Polytechnique de Grenoble, ENS d'Electrochimie et d'Electrométallurgie de Grenoble, BP 75-Domaine Universitaire, 38402 SAINT-MARTIN D'HÈRES, France*

Considering the similarity between graphite and hexagonal boron nitride (h-BN) structures, this study aims to elaborate boron nitride filaments analogous to filamentous carbon. Filamentous carbon is obtained by decomposition of a hydrocarbon coming into contact with a metal belonging to the iron family. Dissolving carbon in this metal leads to the precipitation of filamentous carbon around metallic grains. In the case of h-BN, the metallic phase may be zirconium owing to the solubility of C and N in this metal, although in practice it is easier to use $ZrB_2$. BN filaments were obtained when $B_2H_6$ and $NH_3$ (or $N_2$) came into contact with this compound (or borides of related metals) at temperatures around 1100 °C. Nevertheless it has been shown that BN filaments also occurred in the absence of $B_2H_6$; therefore the boron of the filaments originates in the boride. TEM observations showed that BN filaments exhibit structure, morphology and dimensions ($\phi \sim 0.1$ μm, $L \sim 1$–$10$ μm) analogous to those of C filaments, although the formation mechanisms are different.

## 1. Introduction

Carbon fibres can be prepared by hydrocarbon pyrolysis in the presence of suitable iron particles [1–4]. Vapour-deposited carbon fibres grow by a two-stage mechanism, postulated by Hillert & Lange [5] and verified by several authors [6, 7]:

(i) catalytic lengthening of a tubular carbon filament from a metallic (or carbidic?) particle;

(ii) thickening of the tube by pyrocarbon deposition.

This tubular morphology also occurs in most cases when carbon filaments grow from a carbon-containing gas upon a transition metal [8–11]. It probably originates from the dissolution–precipitation mechanism involved in their growth [12] as the external diameter of the tube is generally close to that of the metallic particle which it appears to issue from. Thus Tibbetts [13] suggested a model allowing the prediction of internal diameters of tubes against their external diameters and emphasizing the difference between the surface energies of graphite basal planes and of "a typical prismatic surface perpendicular to this". Although no growth of microtubes for solids other than carbon had been reported, Tibbetts concluded that "other compounds having highly anisotropic surface free energy could form hollow whiskers".

The purpose of the work reported in this paper is to obtain such filaments with hexagonal BN (h-BN), which is isostructural with graphite. Indeed, boron nitride and carbon are isoelectronic and h-BN is well known to have a layered structure similar to graphite (except that in h-BN the hexagons are stacked directly on top of each other instead of being staggered as in graphite). Therefore it should be possible to obtain boron nitride filaments by transposing to this material the conditions in which carbon filaments deposit from carbonaceous gases in the presence of catalytic particles able to dissolve carbon.

## 2. Experimental procedure

Thermodynamics permits the deposition of boron nitride from a great number of gaseous mixtures containing both boron and nitrogen. Diborane and ammonia or nitrogen were chosen in order to prevent undesirable by-products from depositing. The desired balance could be written:

$$B_2H_6 + 2NH_3 \rightarrow 2BN + 6H_2$$

or

$$B_2H_6 + N_2 \rightarrow 2BN + 3H_2$$

The aim was to find a condensed phase able to dissolve boron and nitrogen simultaneously, as iron and metals of its family are thought to dissolve carbon during the catalytic growth of filamentous carbon. The triangular diagram zirconium–boron–nitrogen [14] exhibits several homogeneous domains, particularly around the metal and around the $ZrB_2$ stoichiometry. Boride was chosen as the catalyst because of the difficulties in handling zirconium powder without oxidizing its surface.

After having obtained positive results with $ZrB_2$, tests were carried out with diborides of different neighbours of Zr in the periodic table: $HfB_2$ (Johnson Matthey Cmbh, Karlsruhe), $TiB_2$ and $VB_2$ (Aldrich

*Also at Université Joseph Fourier, Grenoble, France.

0022–2461 

Chimie, Strasbourg), $NbB_2$ and $TaB_2$ (Goodfellow Metals Ltd., Cambridge, U.K.). Metal boride was laid down on a solid tablet settled in the middle of a cylindrical quartz reactor, placed in a horizontal furnace. The reactor was flown by argon and heated from room temperature to $\sim 1100\,^{\circ}C$. Then argon was replaced by ammonia (linear velocity 4.2 or 2.1 cm $min^{-1}$ before mixing with the other gases) and a mixture of diborane with hydrogen (containing 2 mol % diborane) was introduced by a tube settled inside the reactor and emerging around 1 cm above the diboride. (The flow of hydrogen–diborane mixture was half that of ammonia.) The homogeneous reaction between gases was minimized, in comparison with the desired heterogeneous one, by this geometry and by the choice of a low proportion of diborane. Nevertheless, diborane partially decomposed inside the introducing tube, and the deposited boron may block the tube for experiments longer than 2 h. After this duration, all gases were replaced by argon and the reactor was cooled.

Nitrogen used in this experiment was nominally 99.995% pure and ammonia 99.96%. Because of its toxicity and inflammability, even diluted at 2% in hydrogen, diborane was stored in a ventilated cupboard. Both ($B_2H_6 + H_2$) and $NH_3$ (or $N_2$) flow-rates were monitored by mass flow-meters. Temperature was controlled by a chromel–alumel thermocouple set in a thermowell ending near the solid. After flushing out and cooling of the reactor, some powder was picked up from the tablet and ultra-sound dispersed in ethanol. One drop of this suspension was laid down on an amorphous-carbon-covered copper grid and observed by transmission electron microscopy (TEM) and other techniques.

## 3. Results

Preliminary experiments were performed without any catalyst. A white powder was obtained (Fig. 1). Its amorphous nature was demonstrated by the absence of any peak in X-ray diffraction (XRD). The Infra-red spectrum (Fig. 2) showed that it was boron nitride, i.e. the product of the homogeneous reaction between $B_2H_6$ and $NH_3$.

Further experiments were carried out using $ZrB_2$, $NH_3$ and $B_2H_6$ in accordance with the procedure described above. Solid deposits were analysed by TEM (Fig. 3), which shows: (i) $ZrB_2$ particles with dimensions higher than 1 μm; (ii) small, spherical particles (10 nm < ϕ < 100 nm) identical to those obtained in the preliminary experiments (homogeneously formed BN); (iii) filaments which were identified as BN by electron energy loss spectrometry [15]. In various micrographs, the filament length lies between 1 and 50 μm, whereas their width varies between 0.1 and 0.3 μm. Their tubular structure, similar to that of carbon filaments, was evidenced by moving one of them around its axis without any significant change of the image. The lighter, central part of filaments is clearly apparent in Fig. 4, where a darker spot demonstrates a zirconium-based particle. Such particles were often observed in the tubular core of the filament and more rarely at the top, as for carbon

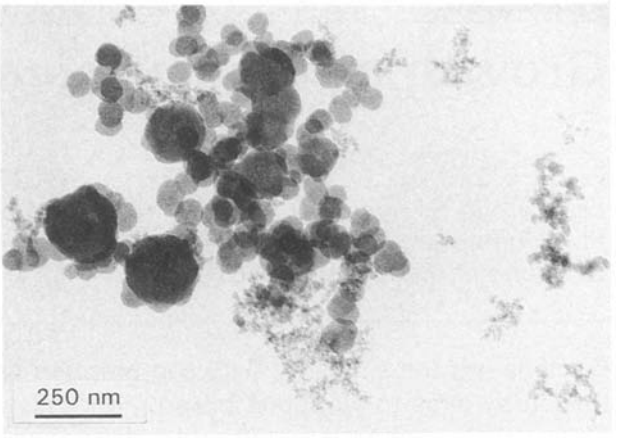


*Figure 1* Amorphous BN powder

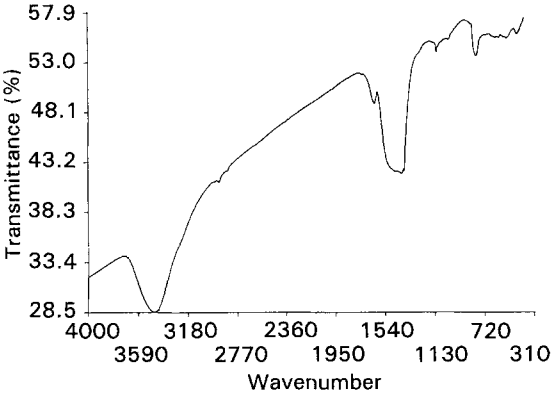


*Figure 2* Infra-red spectrum of BN powder

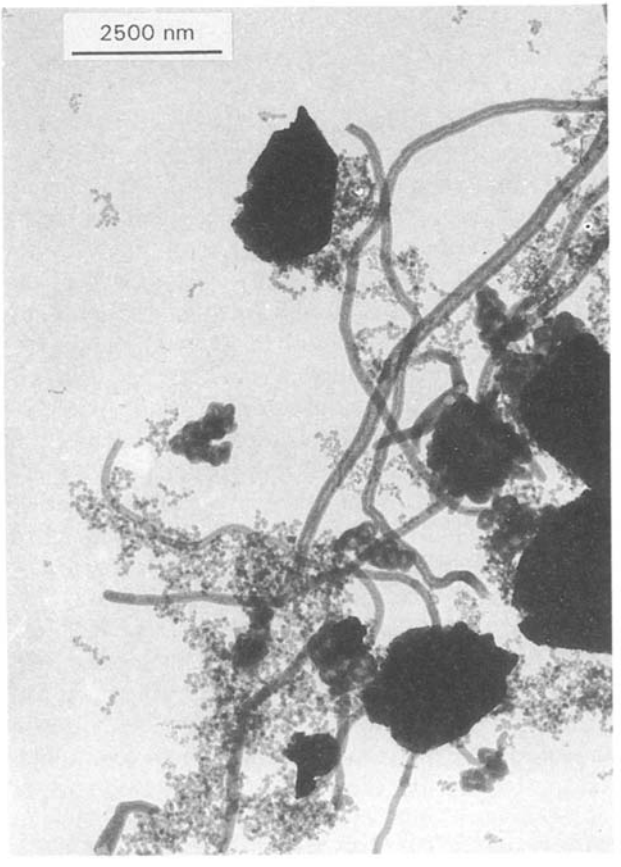


*Figure 3* Product of reaction of $NH_3$–$B_2H_6$ mixture with $ZrB_2$

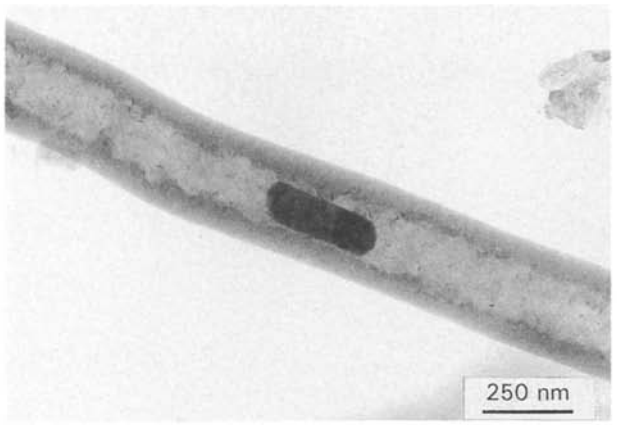


*Figure 4* Hollow BN filament with a zirconium-based particle

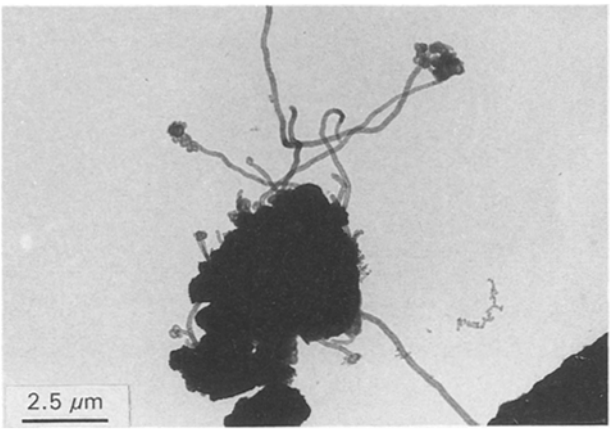


*Figure 5* BN filaments issuing from a $ZrB_2$ grain

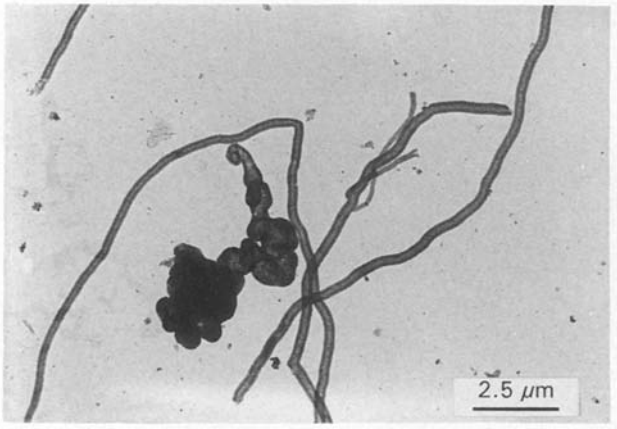


*Figure 6* Product of reaction of pure $NH_3$ with $ZrB_2$

filaments. Fig. 5 suggests that filaments grow from the surface of zirconium boride grains. It was therefore important to understand the role played by $ZrB_2$. In order to separate the reaction of $B_2H_6$ with $NH_3$, and a possible reaction between $NH_3$ and $ZrB_2$, this last compound was heated to 1100 °C under a pure $NH_3$ flow. Unexpectedly, it was observed by TEM that this last reaction leads to the growth of filaments like the previous ones (Fig. 6). On the other hand, in the same experiment without $B_2H_6$, no amorphous BN particles were formed.

Two phenomena are therefore distinguished: (i) a reaction between gases: $B_2H_6 + 2NH_3 \rightarrow 2BN$ (amorphous) $+ 6H_2$, and (ii) a gas–solid reaction involving $ZrB_2$ and $NH_3$. The yield of this second reaction was too low for other products to be unambiguously identified. Besides unreacted $ZrB_2$, $ZrO_2$ (probably issuing from gaseous impurities) and ZrN could be identified on X-ray diffractograms. The chemical reaction leading to the formation of ZrN may be written as:

$$ZrB_2 + 3NH_3 \rightarrow ZrN + 2BN(\text{filamentous}) + \frac{9}{2}H_2$$

One particle inside a filament was identified by selected-area electron diffraction as a ternary Zr, B, N solution which might result from the reaction:

$$ZrB_2 + 2xNH_3 \rightarrow ZrB_{2-x}N_x + xBN(\text{filamentous}) + 3xH_2$$

No experiment could demonstrate that $B_2H_6$ played a role in filament growth. Further experiments were therefore carried out without any diborane; thus the above-mentioned limitation of the experiment duration was no longer necessary. In the case of ammonia, an extension of experimental duration gave no increase of filament yield. Nevertheless extended experiments (72 h) when replacing $NH_3$ by $N_2$ gave filaments (a supplementary extension had no effect on either their number or their length). The shapes (Figs 7–9) of $N_2$-grown filaments differed from the previous one: their length was cut off by occlusions and they were often twisted and wound up. These shapes were commonly observed for filamentous carbon. $N_2$-grown filaments had a length comparable (1–100 μm range) with $NH_3$-grown ones, but they were thinner ($0.01 < \phi < 0.1$ μm). As in the case of $NH_3$-grown filaments, $N_2$-grown ones appeared (Fig. 10) to be extruded from $ZrB_2$ grains according to:

$$ZrB_2 + \frac{3}{2}N_2 \rightarrow ZrN + 2BN$$

$$\text{or } ZrB_2 + xN_2 \rightarrow ZrB_{2-x}N_x + xBN$$

Diborides of different neighbours of zirconium ($TiB_2$, $HfB_2$, $VB_2$, $NbB_2$, $TaB_2$) were then treated in the same conditions, either in ammonia or in nitrogen: (i) 4 h

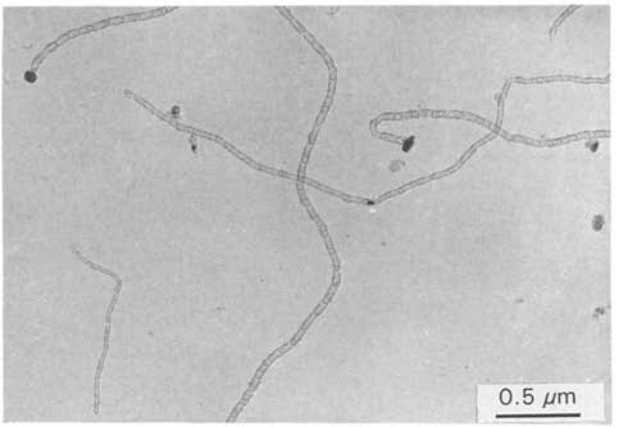


*Figure 7* Product of reaction of $N_2$ with $ZrB_2$

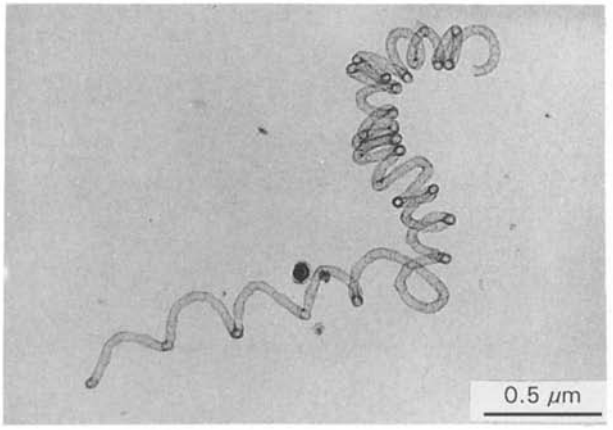


*Figure 8* Coiled filament issued from $N_2$ and $ZrB_2$

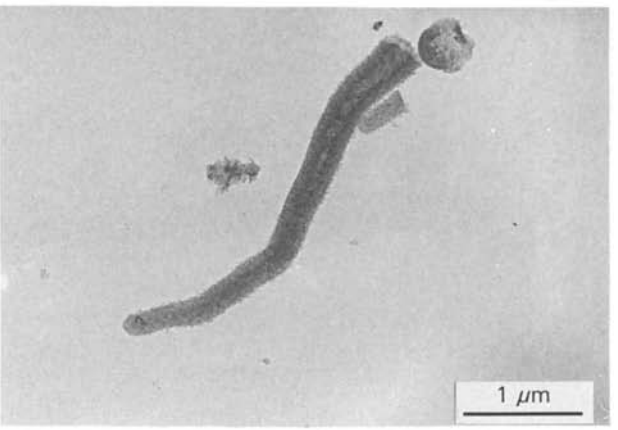


*Figure 11* Product of reaction of $NH_3$ with $HfB_2$

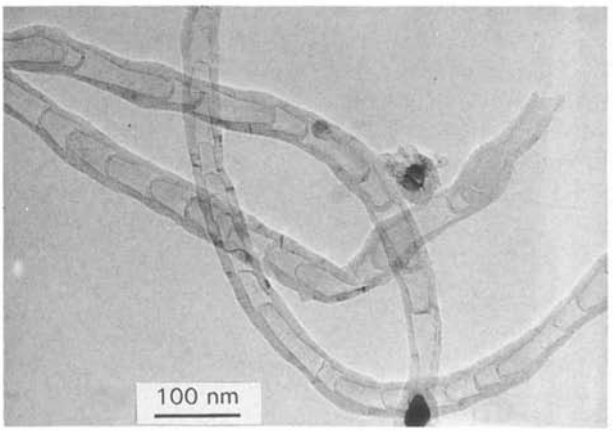


*Figure 9* Part of occlusion-containing filaments

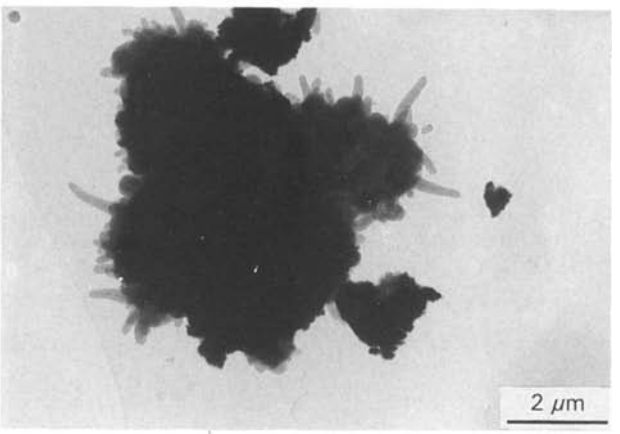


*Figure 12* $NH_3$-grown filaments issuing from $HfB_2$

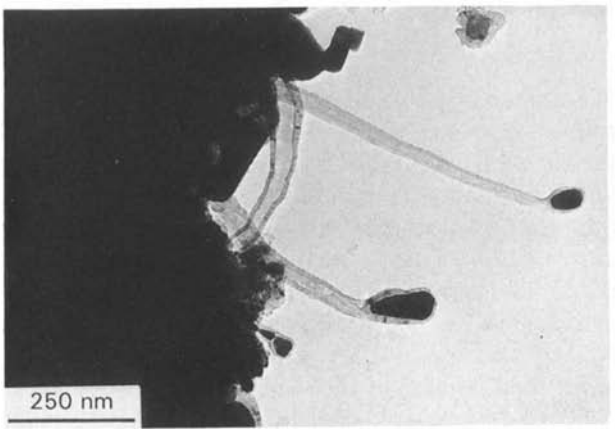


*Figure 10* $N_2$-grown filaments issuing from $ZrB_2$

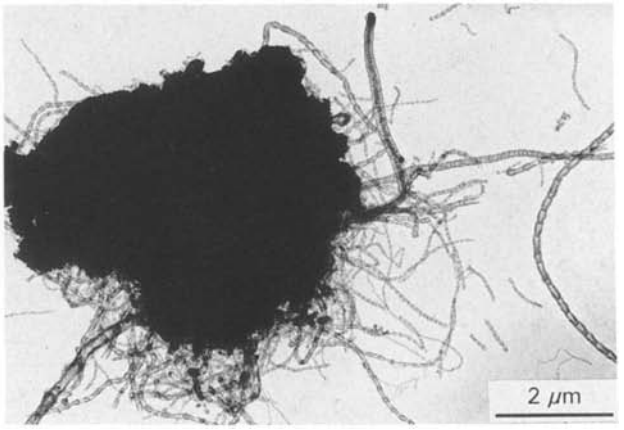


*Figure 13* $N_2$-grown filaments issuing from $HfB_2$

under a 4.2 cm $min^{-1}$ flow of $NH_3$ at 1100 °C; (ii) 72 h under a 4.2 cm $min^{-1}$ flow of $N_2$ at 1100 °C. No filament was grown by using ammonia except with $HfB_2$. In the latter case, filaments (Fig. 11) were shorter than those obtained from $ZrB_2$. Fig. 12 shows that they grew from $HfB_2$ grains. With $N_2$, filaments were obtained from all the considered borides (see for instance Figs 13–15). All filaments obtained with $N_2$ exhibited occlusions.

## 4. Discussion

The appearance of occlusion-containing filaments is not very different from the horsetail-like filaments obtained by Ishii *et al.* [16] (with other morphologies) when heating (to 1500 °C) commercially available hexagonal BN powder "containing considerable amount of oxygen" under nitrogen atmosphere in a tube having a graphite element. The material described by Seon [17] is made of smaller ($L < 1$ μm) and full BN filaments. Except for these two cases, nothing similar to our results has been reported in the literature.

The dissolution–precipitation mechanism which was demonstrated in the case of carbon filaments has obviously to be modified here. Taking into account (i) the appearance of BN filaments originating from


*Figure 14* Scanning electron microscopy of the product of a ($N_2$ + $HfB_2$) reaction

solid grains (Figs 6 and 10), especially from bumps at their surface (Fig. 16); (ii) the fact that the grain surface was demonstrated to be recovered by a BN layer; and (iii) the non-stoichiometric character of $ZrB_2$ or $HfB_2$ [18, 19], the following mechanism may be suggested for the formation of occlusion-containing filaments (Fig. 17):

nitrogen dissolution in $MB_{2-x}$:

$$MB_{2-x} + \frac{y}{2}N_2 \rightarrow MB_{2-x}N_y \; (y \leqslant x)$$

formation of a BN layer:

$$MB_{2-x}N_y \rightarrow MB_{2-x-y} + yBN$$

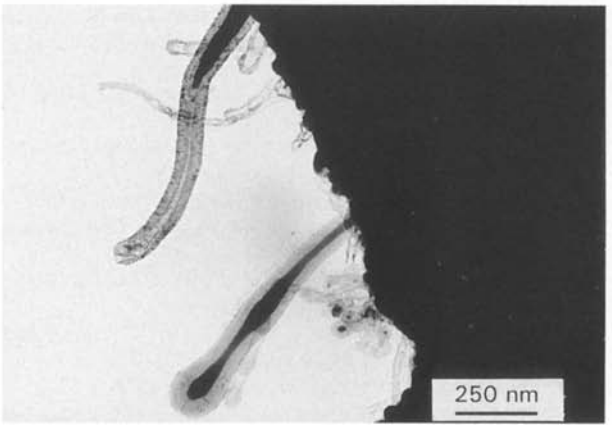


*Figure 15* Some shapes of $HfB_2$-issuing filaments

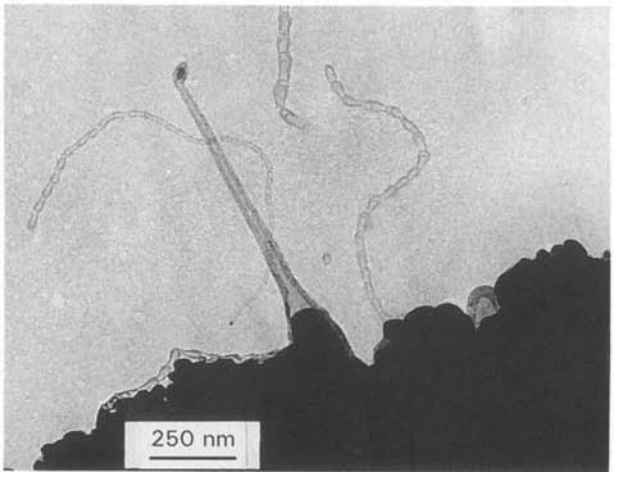


*Figure 16* $N_2$-grown filaments issuing from $HfB_2$ bumps

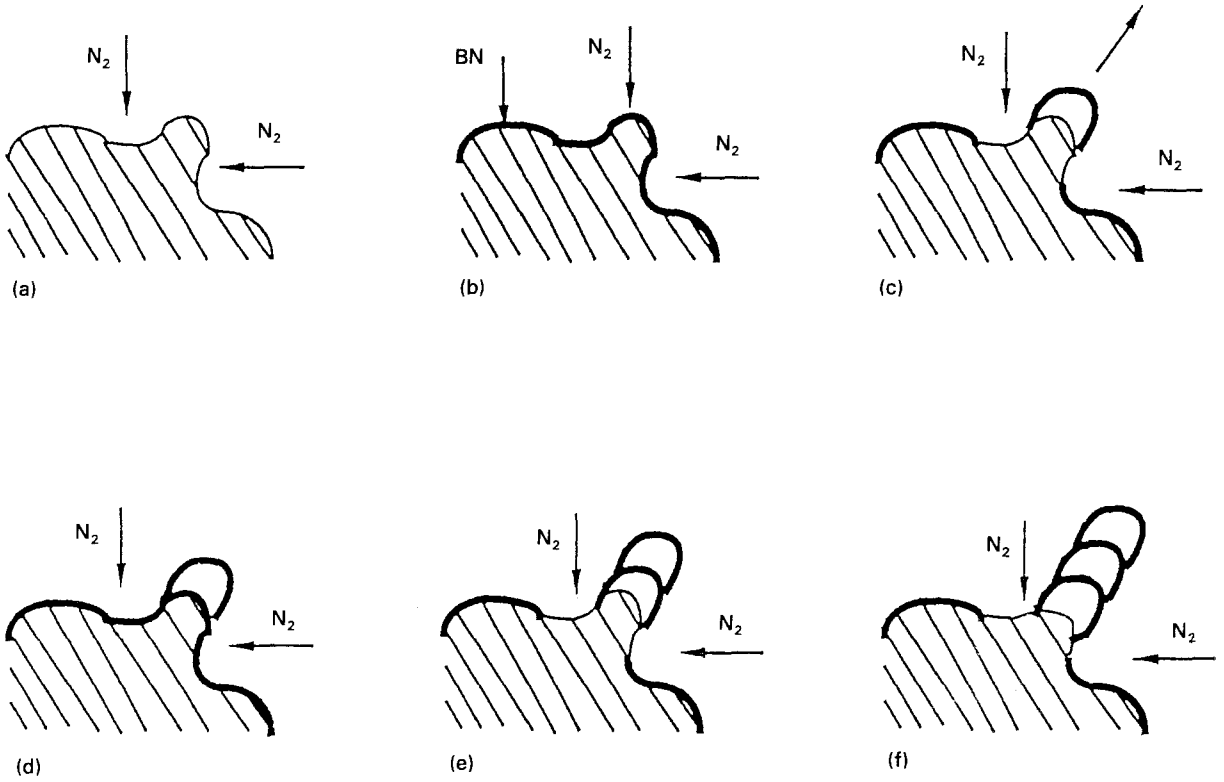


*Figure 17* Proposed mechanism for the growth of occlusion-containing filaments: (a) nitrogen dissolution in $MB_{2-x}$; (b) formation of a primary BN layer; (c) formation of the first cell of a filament; (d) formation of a new BN layer; (e) formation of the second cell of a filament; (f) formation of the third cell of a filament.

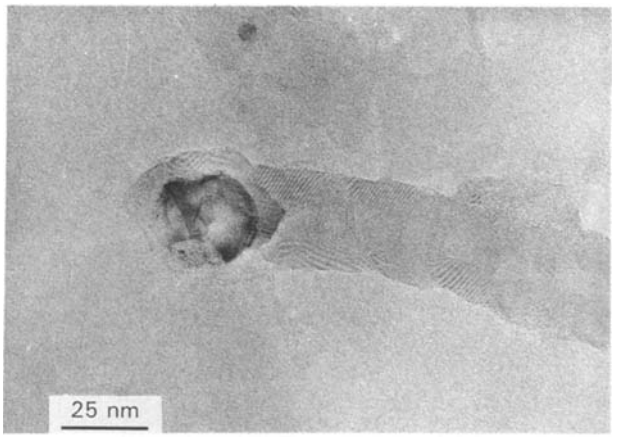


*Figure 18* High-resolution micrograph of a filament issued from a ($N_2$ + $ZrB_2$) reaction

this layer detaches from a bump and becomes a cell of a filament; $N_2$ dissolves again:

$$MB_{2-x-y} + \frac{y'}{2}N_2 \rightarrow MB_{2-x-y}N_{y'}$$

formation of a new BN layer:

$$MB_{2-x-y}N_{y'} \rightarrow MB_{2-x-y-y'} + y'BN$$

this layer detaches from the bump, and so on.

The extent of filament growth would be limited by the amount of boron available, i.e. probably by boron income from the bulk of the grain which would depend upon temperature (solid-phase diffusion), and perhaps the presence of hydrogen (originating from $NH_3$ decomposition). This last hypothesis might explain the differences between experiments performed with $N_2$ and with $NH_3$. Diffusion phenomena in the gaseous phase may also occur, as experiments carried out with lower or higher linear velocities (2 and 6 cm $min^{-1}$ instead of 4) exhibited lower filament yield.

High-resolution transmission electron microscopies (TEM) showed lattice fringes (see Fig. 18 for $ZrB_2$ + $N_2$ filaments). These originate from interference of the scattered 0 0 2 beam (when aromatic layers of BN fulfill the Bragg condition) with the undeviated transmitted 0 0 0 beam. As TEM Bragg angles are less than one degree, aromatic layers seen on the micrograph are almost perpendicular to it. As in the case of vapour-grown carbon filaments, aromatic layers appear bent to truncated cones rather to cylinders (compare Fig. 18 of this paper with Fig. 4 of [9]). Notice that the model of graphitic layers bent to cylinders [13], which is a rough approximation of reality in both cases of carbon and BN vapour-grown filaments, appears accurate in the case of carbon needles recently elaborated by an arc-discharge and observed by high resolution TEM [20].

## 5. Conclusions

Tubular boron nitride filaments were obtained, observed by TEM and demonstrated by EELS [15]. Their morphology and structure suggest vapour-grown carbon filaments, but their growth mechanism differs from that of carbon, as boron is supplied by the metallic boride initially expected to be a catalyst. For practical applications, their growth process should be improved in order to lengthen and thicken them, as when carbon filaments grow up to fibre dimensions [21]. Boron nitride fibres, like massive hexagonal boron nitride, should have a better resistance to oxidation than carbon fibres, and might also be useful owing to the specific properties of BN as a heat conductor and electrical insulator.

## References


1. M. ENDO and K. KOMAKI, in Proceedings of the 16th Biennial Conference on Carbon, San Diego, June 1983 edited by R. J. Price and G. B. Engle (American Carbon Society) p. 523.
2. M. COULON, N. KANDANI, L. BONNETAIN and J. MAIRE, French Patent N° 84.06365 (1984).
3. J. R. BRADLEY and G. G. TIBBETTS, *Carbon* **23** (1985) 423.
4. F. BENISSAD, PhD Thesis, Grenoble, 1986.
5. M. HILLERT and N. LANGE, *Z. Krist.* **24** (1958) 111.
6. A. OBERLIN, M. ENDO and T. KOYAMA, *J. Cryst. Growth* **32** (1976) 335.
7. F. BENISSAD, P. GADELLE, M. COULON and L. BONNETAIN, *Carbon* **26** (1988) 61.
8. R. T. K. BAKER and P. S. HARRIS, in "Chemistry and Physics of Carbon", Vol. 14, edited by P. L. Walker, Jr, and P. A. Thrower (Marcel Dekker, New York, 1978) p. 83.
9. M. AUDIER, A. OBERLIN, M. OBERLIN, M. COULON and L. BONNETAIN, *Carbon* **19** (1981) 217.
10. A. SACCO, Jr., in "Carbon Fibers, Filaments and Composites", edited by J. L. Figueiredo, C. A. Bernardo, R. T. K. Baker and K. J. Huttinger (Nato Asi Series Vol. 177, Kluwer, Dordrecht, 1989) p. 459.
11. G. A. JABLONSKY, F. W. GEURTS, A. SACCO Jr. and R. BIEDERMAN, *Carbon* **30** (1992) 87.
12. M. AUDIER and M. COULON, *ibid.* **23** (1985) 317.
13. G. G. TIBBETTS, *J. Cryst. Growth* **66** (1984) 632.
14. E. RUDY and F. BENESOVSKY, *Mon. Chemie* **92** (1961) 424.
15. P. GLEIZE, S. HERREYRE, P. GADELLE, M. MERMOUX, N. C. CHEYNET and L. ABELLO, submitted to *J. Mater. Sci. Lett.*
16. T. ISHII, T. SATO, Y. SEKIKAWA and M. IWATA, *J. Cryst. Growth* **52** (1981) 285.
17. F. SEON, French Patent N° 88-08579 (1988).
18. L. BSENKO and T. LUNDSTROM, *J. Less-Common Metals* **34** (1974) 273.
19. P. ROGL and P. E. POTTER, *CALPHAD* **12** (1988) 191.
20. S. IIJIMA, *Nature* **354** (1991) 56.
21. P. GADELLE, in "Carbon Fibers, Filaments and Composites", edited by J. L. Figueiredo, C. A. Bernardo, R. T. K. Baker and K. J. Huttinger (Nato Asi Series Vol. 177, Kluwer, Dordrecht, 1989) p. 95.


*Received 13 November 1992*
*and accepted 7 June 1993*